Numerical Study Of Microorganisms In Shear Flows

Engineering Sciences
Department of Engineering Mechanics

Mansoor Ahmed

Master thesis
Department of Engineering Mechanics, KTH,
Stockholm, Sweden 2011

Engineering Sciences

Department of Engineering Mechanics

Numerical Study Of Microorganisms In Shear flows

Mansoor Ahmed

Supervisor: Dr. Luca Brandt

March, 2011

Contents

Preface

The work presented was done as a master's thesis under the supervision of Luca Brandt in the Department of Engineering Mechanics at the Royal Institute of Technology (KTH), Stockholm.

The thesis comprises six chapters. The first chapter is the introduction. The second chapter contains the literature review. Equation used for fluid and the swimmers are provided in chapter 3. Chapter 4 explains the numerical techniques in the analysis done during this thesis while chapter 5 gives the results and discussions and chapter 6 is about the conclusion of the work.

KTH, March 2011

Mansoor

Acknowledgement

I am obliged to my supervisor for his support and guides during this thesis. I feel deeply grateful to all those who supported me to complete this thesis.

I want to pay thank to my parents for their love, prayers, moral and the financial support. I am thankful to my brothers and sister who supported me through some very difficult times. Much too often I felt no strength for carrying on other than their love and encouragement.

KTH, March 2011

Mansoor

Abstract

This thesis is concerned with the numerical study of swimming of microorganism in shear flows. The problem is approached by direct numerical simulation (DNS) and Lagrangian particle tracking (LPT) for the fluid and particle phase. This numerical study is focused on dense swimmers in the solution at moderate values of turbulent Reynolds number. We track the swimmers in Lagrangian frame for turbulent open channel flow at Re_τ = 74.243 and Re_τ = 180 for turbulent close channel flow. We also studied the swimmers in laminar flow at Re_τ = 44.723 for close channel. For all cases we have one way coupling so the swimmers cannot affect the flow behavior. We chose the swimmers with and without gyrotaxis having different shapes. For open channel, we investigate the concentration and orientation of swimmers across the channel. For close channel, we looked at the concentration and dispersion velocity of swimmers in horizontal and vertical channels with gravity in the same and opposite to the direction of flow.

Chapter 1

1.1 Introduction

The trajectory of swimming microorganisms can be determined by the advection of flow. The orientation of their swimming velocity vector with respect to the direction of flow altered in response to number of different internal and external factors [1]. In this thesis we studied the suspension of passive swimming particles in an open and close channel flow. The statistics of organisms are examined by varying the swimming speed of cells, their aspect ratio and with and without gyrotaxis at different resolutions in an open and close channel.

For example, consider a typical algal cell, Chlamydomonas, has shape approximately spheroid with a pair of flagella at one end and due to this cell swims in a direction roughly parallel to its axis. These cells are bottom heavy and tend to swim upwards due to the anisotropic mass distribution of organelles within their cell body. If they start to swim at an angle to the vertical, the gravitational couple would immediately rotate them to the vertical. However, if the fluid medium flows with the horizontal component of vorticity, it will exert the viscous torque on the cell and rotate it away from the vertical. If the vorticity is not too large, there will be a balance between the viscous and gravitational torques, and the cell swim at a fixed angle θ to the vertical. This mechanism of cells movement is called gyrotaxis.

$$\sin\theta = B\omega \qquad \textbf{Equation 1-1}$$

Where "ω" is the horizontal component of vorticity in the flow and "B" is the constant that is determined by the geometry of the cell and viscosity of the suspending fluid.

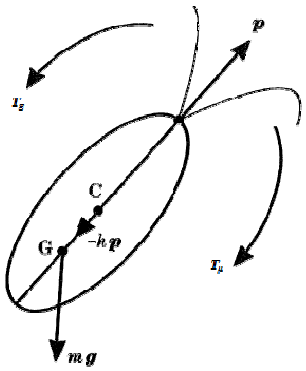

Figure 1-1

Figure 1-1 shows such a cell placed in a shear flow. where "p" is the unit vector in the swimming direction, "h" is the displacement of the center of gravity "G" from the center of the cell "C", so that $\mathbf{h} = h\left(\hat{x}\sin\theta - \hat{y}\cos\theta\right)$ relative to the Cartesian coordinates, The force of gravity, acting through the centre of mass exerts a torque $T_g = mh \times g$, where m is the mass of the cell and g is the acceleration due to gravity. The viscous torque on a spherical cell of radius 'a' in a fluid of viscosity μ is given by

$$T_\mu = 4\pi\mu a^3(\nabla \times u - 2\Omega) \qquad \textbf{Equation 1-2}$$

Where ***u*** is the fluid velocity field and Ω is the cell's angular velocity. The rate-of strain tensor gives rise to an additional torque only on non spherical bodies. Hence the total torque is given by

$$T = 4\pi\mu a^3(\nabla \times u - 2\Omega) + mh \times g \qquad \textbf{Equation 1-3}$$

1.2 Microorganisms

The term **organism** represents an individual that is capable to grow, metabolize nutrients, and usually able to reproduce. It can be unicellular or multicellular. Organisms which are so small and invisible to the naked eye constitute microorganisms. If any object is smaller than 0.1 mm, the human eye can not perceive it and even at a size of 1.0 mm very little details of an object

can be seen with the naked eye. Organisms are divided into five different groups named prokaryotes, protists, fungi, plants, and animals. These groups are also called kingdoms. [3]

1.3 What is Taxis?

Taxis is a Greek word which means arrangement. According to Henderson's dictionary of biological terms its definition is

"A movement of free motile, usually simple organisms, especially Protista, or part of an organism. Towards (positive), or away from (negative), a source of stimulation, such as light, temperature, chemicals; an orientation behavior related to a directional stimulus."

Taxes include change in surroundings and mechanisms of organism's movement in response to that change in surroundings. Organisms move in random manner in the absence of taxes. Most organisms use a combination of random movement and taxes. Natural selection ensures that optimal tactics are always employed.

There are some typical examples of taxis:

Chemotaxis: in this, organisms move towards or opposite to the chemical concentration gradient. Chemotactic bacteria experience the change in nutrient concentration with time. If there is any change in sensed concentration level, they respond by appropriate change in their tumbling probability.

Phototaxis: In this, organisms are sensitive to light intensity, its direction or polarization. Phototactic organisms need light for photosynthesis so they swim towards it.

Geotaxis: In this, organisms move towards or opposite to the gravity. This is also known as gravitaxis. Organisms those are bottom heavy tend to move upwards due to anisotropic mass distribution of organelles within their bodies. This upward movement is known as negative gravitaxis or negative geotaxis.

The orientation of organisms is due to gradients in local fluid velocity. Their swimming is vorticity sensitive. The rotational viscous drag and the distance between the center of volume

and the center of mass are responsible for the angle between the axis of the cell and the vertical direction. Swimming by this mechanism is termed as **gyrotaxis**.

Rheotaxis: In this, organisms try to keep position in a stream rather than being swept downstream by the flow because of their shape. Some organisms exhibit negative rheotaxis where they will avoid flow.

Microorganisms need any mechanism to come close for sexual mating. So chemotaxis can effectively drive sexual aggregation. Geotaxis and gyrotaxis result in pattern formation. In the absence of wind shear or thermal convection, gyrotaxis might work to extract more nutrients from the bed of a pond than a mere geotactic instability, involving organisms that do not exhibit gyrotaxis, by increasing the width of up flowing fluid and creating higher wall shear stress.

1.4 Wall bounded Flows

By definition Turbulent flow is not stationary but stationary in the mean i.e. fluctuating around the mean value. The fluid motion is irregular and shows a random variation in both space and time. The flow field should show large vorticity intensity and vortices should span over a large range of scale.

Turbulent flows are categorized into **internal flows** and **external flows**. Fully developed flows through pipes and ducts are common examples of internal flows. In these flows mean velocity profile and friction laws are of important concern which illustrate the shear stress exerted on the wall by the fluid. External flows include flow around aircraft and ships etc.

Boundary layer flows are complex as compared to flows in free shear layers because, walls present in bounded flows imposes constraint for example viscosity of the fluid causes no slip condition. This no slip condition or viscous constraint that causes a viscosity characteristic length of the order of υ/w where υ is the kinematic viscosity and w represents characteristic of the level of turbulent velocity fluctuations. At high Reynolds numbers, υ/w is smaller than boundary layer thickness δ, so we can say that υ/w will not influence the entire flow.

Friction velocity

$$u_\tau = \sqrt{\frac{\tau_w}{\rho}} \qquad \textbf{Equation 1-4}$$

Viscous length scale

$$l_* = \frac{\nu}{u_\tau} \qquad \textbf{Equation 1-5}$$

The Reynolds number defines on the basis of viscous scales

$$\mathrm{Re}_\tau = \frac{u_\tau \delta}{\upsilon} = \frac{\delta}{\upsilon / u_\tau} = \frac{\delta}{l_*} \qquad \textbf{Equation 1-6}$$

The percentage of viscous stress to the total stress decreases from 100% at the wall where $y^+ = 0$ to the 50% at $y^+=12$ and less than 10% by $y^+=50$.

$$\tau(y) = -\rho\langle u'v'\rangle + \mu\frac{\partial U}{\partial y} \qquad \textbf{Equation 1-7}$$

Where $-\rho\langle u'v'\rangle$ represents the Reynolds stress and $\mu\frac{\partial U}{\partial y}$ viscous stress.

We divide the regions near wall on the basis of y^+.

In 1925 Prandtl postulated that in ***inner layer*** u^+ is only the function of y^+ for $y/\delta << 1$.

$$U^+\left(y^+\right) = y^+, \qquad y << \delta \qquad \textbf{Equation 1-8}$$

In ***viscous sub layer***, the deviation from the linear relation $u^+=y^+$ are negligible for $y^+<5$, but significant for $y^+ > 12$.

The log law or the logarithmic law of wall due to von Karman

$$U^+\left(y^+\right) = \frac{1}{k}\left(\ln y^+\right) + B \qquad \textbf{Equation 1-9}$$

Where “k” is von Karman constant and “B” is the constant of integration. In the literature, there is little variation in the values of these constants, but generally these are within 5%.

K = 0.41 and B=5.2

Buffer layer, is the region between viscous sub layer ($y^+ < 5$) and log-law region ($y^+ > 30$). It is transition region between viscosity-dominated and turbulence-dominated parts of the flow.

In the ***outer layer*** where velocity profile is not expected to depend on the viscosity for high Reynolds numbers.

$$U(y) = U_o - u_\tau \Psi_1(Y, \mathrm{Re}_\tau), \qquad y >> l_* \qquad \textbf{Equation 1-10}$$

Where $Y = \frac{y}{\delta}$

1.5 Isotropic Turbulence

Kolmogorov’s idea is that the parameters those are responsible for the size of dissipating eddies are relevant to the smallest eddies. These parameters are the rate of energy dissipation ϵ and the viscosity υ that does the smearing out of the velocity gradients. In turbulent flow at high Reynolds number, the statistics of the small scale motions have universal form those can be determined by ϵ and υ.

With these parameters we can form length, time and velocity scales.

$$\eta = \left(\frac{\upsilon^3}{\varepsilon}\right)^{\frac{1}{4}} \qquad \textbf{Equation 1-11}$$

Where “η” is the kolmogorov’s length scale

$$t_\eta = \left(\frac{\upsilon}{\varepsilon}\right)^{\frac{1}{2}} \qquad \textbf{Equation 1-12}$$

$$v_\eta = (\upsilon\varepsilon)^{\frac{1}{4}} \qquad \textbf{Equation 1-13}$$

We considered these length, time and velocity as the smallest length, time and velocity scales respectively in our problem. For channel flow, these scales vary as the distance from the wall varies. To find the swimming speed of micro-organisms we used the Kolmogorov's velocity scale.

Chapter 2

Literature Review

In recent years, the interest to investigate spontaneous pattern formation in suspensions of motile microorganisms is increased. These organisms are evolved million of years ago wether they are in our stomach or affecting the global weather by photosynthesis in the sea. They form certain patterns which is definitely an important part of their life. It is crucial that we understand how and why these organisms, at the base of the whole food chain, behave. After all, they consist of the majority of the Earth's biomass and variation in their numbers could have a catastrophic consequences e.g. positive or negative feedback effects in global warming.

There is also the possibility of harnessing the power of microorganisms. Some algae and bacteria produce alcohol as an unwanted byproduct but to us this is a valuable commodity not least for its use as a fuel, plastics, fertilizers, waste treatment plants and solid fuels are other possible applications for algae and their products. Aim of this thesis is to explain the patterns observed in suspensions of swimming microorganisms.

Fluid flow is affected by the microbes, these microbes act as point source of gravitational force in the fluid equations. Swimming speed and direction are affected by the physical factors e.g. vorticity and gravity, and the sensory factors. To use microbes as point particles allows the variation of input parameters and modeling, while performing calculations with very large number of particles so the realistic cell concentrations and macroscopic fluid effects can be modeled with one particle representing one microbe. Variety of external factors including nutrient concentration, gravity, and the vorticity and the rate of strain of the fluid affect the orientation of its swimming velocity vector relative to embedding fluid. The angle between the axis of the cell and the vertical direction depends upon the rotational viscous drag and the distance between the centre of volume and the centre of mass. In the case of gyrotactic microbes, the swimming orientation is a function of the gradients of the fluid velocity field. A discrete representation of microbes is adopted; do not seek to capture in detail the geometry. Incompressible and homogenous fluid is assumed and very small volume fraction of microbes

which have negligible effect on the viscosity and inertia of the fluid-microbe suspension. When the geotaxis torque is coupled with the torque due to vorticity, two different affects can occur. Microbe rotates “end-over-end” at a uniform rate if the geo-orientation response may overcome by the large value of torque due to vorticity. At smaller turning moments, the torques balance at some intermediate orientation. If a neutrally-buoyant cell is bottom heavy it will tend to swim vertically upwards in the absence of any other stimuli resulting in negative “gravitaxis”. Such cells are also gyrotactic in that a local velocity gradient will produce viscous torques on the cell’s body tending to tip it away from the vertical. [7]

Gyrotaxis can be established in an experiment, a vertical tube of circular cross section is used for a slow Poiseuille flow down. The balance between viscous torques and gravitational torque gives one stable equilibrium orientation with individual cells tipped away from the upward vertical towards the axis of the pipe. If cells are carried along in the pipe they swim towards the axis, and accumulate into a narrow beam. Conversely, they are oriented away from the axis toward the walls if the direction of the flow is reversed, confirming the role of gyrotaxis in cell orientation. If the cell is the most bottom-heavy possible, i.e., the center of mass is at the circumsphere, the value of B would be approximately 0.14s. On the other hand, if the cell becomes less bottom-heavy, the value of B increases and ultimately becomes very large. For small values of G (more bottom heavy cells), the cells swim upwards preferably and are less prone to focus laterally into the plume. If the value of G is large (less bottom-heavy cells) the viscous torque exceeds gravitational torque and as a result the cells tend to tumble. [8]

Some extra stresses contribute to the bulk deviatoric stress tensor due to swimming of cell. The only significant addition to the bulk deviatoric stress tensor, other than the Newtonian stress, is the derived from the stresslets associated with the cells’ intrinsic motions when the suspension is dilute. Generalized Taylor dispersion theory is used to calculate this extra stress term but not complete theory exists for all flows. To make realistic computational progress, the stress associated with the cells’ locomotion is neglected. Inertial effects are negligible at the low Reynolds number flow associated with the motion of the cells, their orientation is specified by

T_g+T_μ =0 and leads to the equation for reorientation rate. Due to strong circulation at the bottom boundary cells remain at the bottom after reaching there, if the value of G is large. [9]

Fluid flow is governed by the Navier–Stokes equations with a negative buoyancy term to represent the effect of the cells on the fluid (Boussinesq approximation). Explicit results for several useful cases are presented from the Taylor–Aris limit to fully coupled gyrotactic spherical swimming cells (i.e. cells that drive the flow and whose swimming direction is biased by external and viscous torques). The expressions reveal the mechanisms for several competing effects and explain how these lead to diffusion and (positive or negative) drift through the tube. Fundamentally, the cells swim and, in the limit that they are very bottom heavy, they may swim mostly against a down welling flow, leading to a negative drift relative to the mean flow. On the other hand, cells those are not bottom heavy act more like diffusing passive tracers, with no drift. In both these cases, the cells diffuse as a balance between gravitational and viscous torques, a balance that will vary across the pipe flow, can lead the cells to form gyrotactic plumes, inducing further flow and self-concentration. These centrally focused plumes of cells can be strongly advected with the flow (i.e. faster than the mean flow) but will sidestep classical shear-induced Taylor-Aris dispersion; effective diffusion may be dominated by swimming diffusion, even for large flow rates. It is clear that swimming behavior leading to drift across streamlines can have a tremendous influence on cell transport in such systems. [10]

Whether the flow in tubes is laminar or turbulent, gyrotactic swimming cells are organized in patterns that alter the flow. It is well known that the transition to turbulence in a tube is strongly sensitive to the initial laminar state. It is interesting to note that the perturbation by the presence of swimming cells should inevitably change the onset of the transition. Cells in turbulent flows in pipes have not been analyzed, but Lewis showed that gyrotactic algae in a homogeneous and isotropic turbulent flow field retain their bias. Turbulence only changes the effective value of the diffusivity of cell orientation. [11]

In almost all cases known to us the only relevant body force is gravity which operates whenever the average density $\rho + \Delta\rho$ of the cell differs from ρ of the ambient fluid; in this case $F = g\Delta\rho/\rho$,

where g is the gravitational acceleration. A cell that is not swimming and for which $\Delta\rho$ is nonzero will have a terminal or sedimentation velocity V_t. In most cases of interest, the magnitude of V_s is much greater than that of V_t and sedimentation may be neglected while the cell is swimming. Most cells also rotate as they swim. At any instant, then, the sum of the total effective external torque L and the viscous torque L_v exerted by the ambient fluid must be zero. If L is zero and the cell is not swimming then it will rotate with a time-dependent angular velocity Ω that depends linearly on the ambient vorticity ω and strain-rate E, as analyzed for ellipsoidal bodies. If the cell is swimming then the angular velocity is likely to be modified. If L is nonzero and the ambient fluid is at rest, then the cell must either rotate or activate its swimming apparatus to generate an equal and opposite L_v. However, if L and the ambient velocity gradient are both nonzero, it is possible for the cell to have zero angular velocity or in other words a fixed swimming direction. Many microorganisms appear to swim, on average, in a given direction, k say, when the ambient fluid is at rest. This suggests that, if p were not parallel to k, the body would experience an effective external couple tending to reduce the angle between them. For a general rigid body at zero Reynolds number, the viscous torque L_v can be written as a linear combination of the velocity and angular velocity of the body relative to the fluid and of the strain rate. For a swimming cell the details of the flagellar or ciliar motions will also be important but their effect on L_v has as yet been analyzed only for spermatozoa with helically beating flagella in a fluid otherwise at rest. Most of the interesting effects to be discussed can be understood if we treat a cell as a rigid prolate spheroid whose axis of symmetry is aligned with p. for the case in which L is gravitational B was called the "gyrotactic orientation parameter". The component of the torque balance equation parallel to p merely states that the component of the cell's angular velocity in that direction is the same as that of the ambient fluid. In a steady but nonuniform velocity field, a cell's orientation will change gradually with time-assuming that a stable equilibrium orientation exists for each spatial location-because as it swims the cell's trajectory will take it to different locations where the vorticity and strain rate are different. Computations of the trajectories of individual cells, still neglecting random effects, have been made for spherical cells ($\alpha o = 0$) in downwards pipe flow. [12]

Chapter 3

3.1 Particle laden Flow

Particle laden flow is a flow in which particles are dispersed. This makes it a two phase flow, the fluid forms the continuum phase while the particles form the dispersed phase. Multiphase flows have more complicated dynamics as compared to the single phase flow. Single phase flow can be characterized solely by the Reynolds number, but to characterize the two phase flow we need volume fraction of particles "Φ_p" and Stokes number "S_t". These non-dimensional numbers are defined as

$$\Phi_p = \frac{NV_P}{V} \qquad \textbf{Equation 3-1}$$

$$S_t = \frac{T_p}{T_s} \qquad \textbf{Equation 3-2}$$

Where

N, V_p, V, T_p, T_s, represent the number of particles, the volume of a single particle, the total volume occupied by both phases, the characteristic time scale of the turbulent flow and the friction time scale considered for wall bounded respectively.

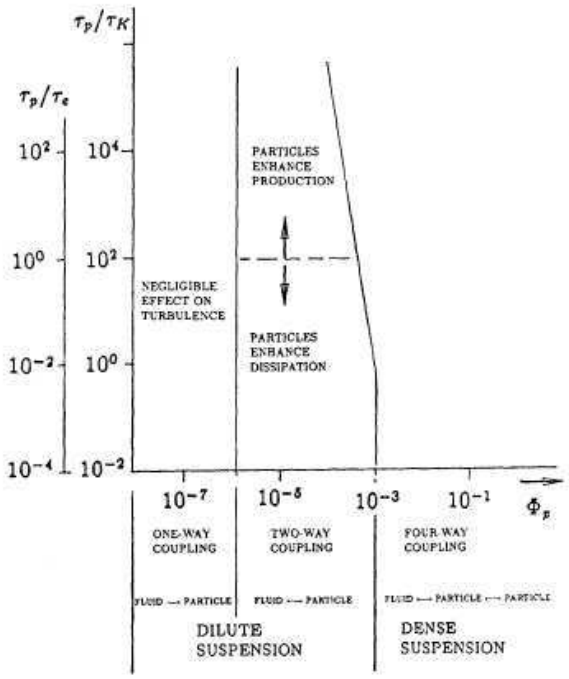

Figure 3-1

For small Φ_p, the particles have negligible effect on the turbulence, and the interaction between particles and turbulence is termed as one way coupling. In such cases particle dispersion will depend only on the state of turbulence. If the value of Φ_p increases, the momentum transfer from the particles is large enough to change the turbulence structure. This is known as two way coupling. For very high value of Φ_p in addition to the two way coupling, particle-particle collision takes place, which is called four way coupling. In our simulations, we have low stokes drag, low inertia and passive particles so we have the case of one way coupling.

3.2 Physical Model

3.2.1. For Open Channel

For open channel flow, we have constant pressure gradient. We have the periodic boundary conditions in “X” and “Z”, stress free boundary condition at upper boundary and no slip boundary condition at lower boundary. We have elastic collision for particle-wall interaction.

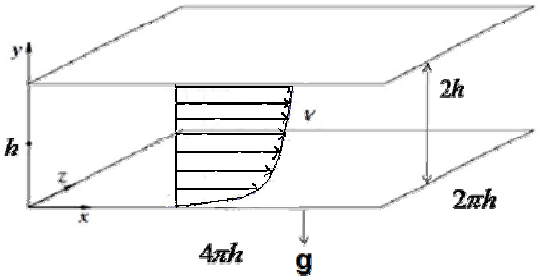

Figure 3-2

Parameters Used for Open channel

Parameter	Values	Description
l_x x l_y x l_z	4π x 2 x $\frac{4\pi}{3}$	Channel dimensions
n_x x n_y x n_z	192 x 129 x 192 128 x 129 x 128	Resolution for Turbulent
α	0.0 0.8,0.9 1.0	Spherical Ellipsoid Elongated
V_s	0.02, 0.04 and 0.05	Velocity of Swimming Particles
Re	2100	Reynolds Number(Turbulent)
Re_τ	74.246	Friction Reynolds Number (Turbulent)
npart	512000	Number of particles
G	0.147	Gyrotaxis

Note: Data non-dimensional with half-channel height and centerline velocity for laminar flow

3.2.2. For Close Channel

For closed channel flow, we have constant mass flux, periodic boundary conditions in "X" and "Z" and no slip boundary condition on upper and the lower walls. We have elastic collision for particle-wall interaction. In the figures 3-2 and 3-3, we showed all the models those we used for closed channel cases. For all models length of the channel is considered along the x-axis, height of the channel is along the y-axis and width of the channel along the z-axis. In figure 3-2 the channel is horizontal and the direction of gravity is in negative "y" direction. In figure 3-3(a) the channel direction is vertical and gravity is in negative "x" direction so the flow is against gravity and In figure 3-3(b) the channel direction is vertical and gravity is in positive "x" direction and the flow is in the direction of gravity.

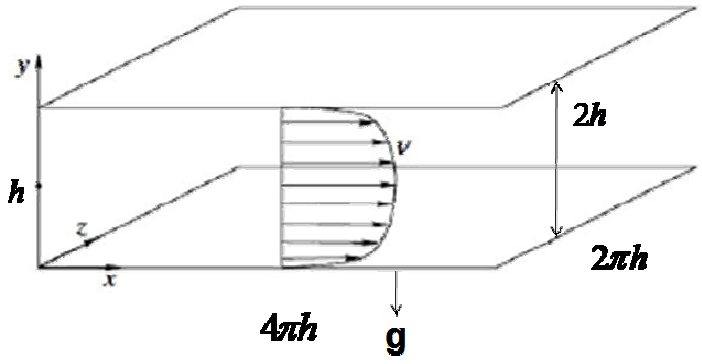

Figure 3-2: Horizontal channel with direction of gravity in negative "y" direction.

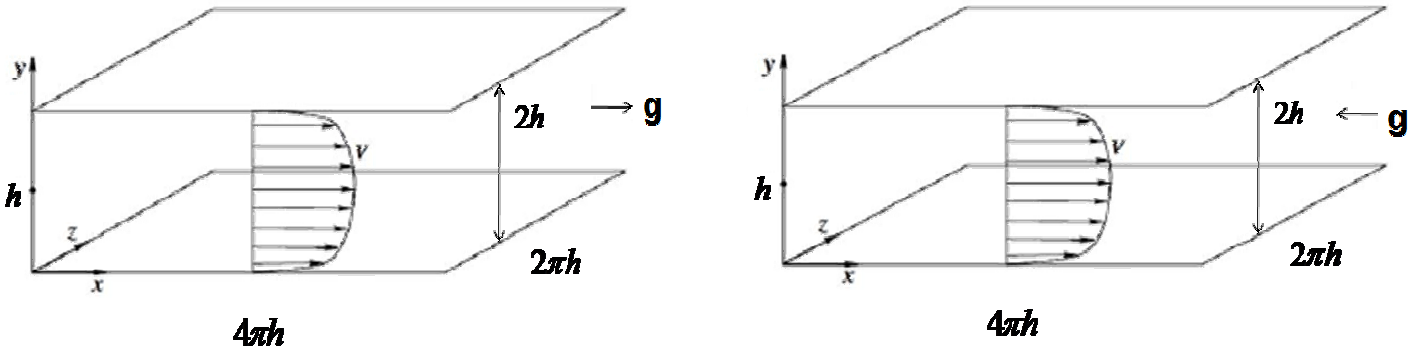

Figure 3-2: (b) Vertical channel with gravity in negative "x" direction. (c) Vertical channel with gravity in positive "x" direction.

Parameters Used for Close Channel

Parameter	Values	Description
l_x x l_y x l_z	4π x 2 x $\frac{4\pi}{3}$	Channel dimensions
n_x x n_y x n_z	128 x 129 x 128	Resolution for Turbulent
n_x x n_y x n_z	4 x 129 x 4	Resolution for Laminar
α	0.0 0.8	Spherical Ellipsoid
V_s	0.02	Velocity of Swimming Particles
Re	4200 1000	Reynolds Number(Turbulent) Reynolds Number(Laminar)
Re_τ	180 44.72	Friction Reynolds Number (Turbulent) Friction Reynolds Number (Laminar)
npart	512000	Number of particles
G	0.0833,0.05,0.01 0.073,0.1 0.35	Gyrotaxis for Turbulent Gyrotaxis for Laminar

Note: Data non-dimensional with half-channel height and centerline velocity for laminar flow

3.3 Equation of Motion

Equation of motion of spherical particles in turbulent flows has been developed and presented in literature. These particles are small as compared to the smallest characteristic scale of the flow. We have to stoke drag equal to zero. Corrsin and Lumley proposed the following equation of motion for small sphere with radius "a" and mass "m_p" moving with speed V(t) with its centre located at Y(t)

$$m_p \frac{dV_i}{dt} = m_f \left(\frac{Du_i}{Dt} - \nu \nabla^2 u_i \right) \Big|_{Y(t)} - \frac{1}{2} m_f \frac{d}{dt}\{V_i(t) - u_i[Y(t),t]\}$$
$$- 6\pi a \mu (V_i(t) - u_i[Y(t),t]) - 6\pi a^2 \mu \int_{-\infty}^{t} d\tau \frac{d/d\tau \{V_i(\tau) - u_i[Y(\tau),\tau]\}}{[\pi\nu(t-\tau)]^{1/2}} \quad \textbf{Equation 3-3}$$
$$+ (m_p - m_f) g_i$$

Where $u_i(x, t)$ is the mass of the fluid displaced by the sphere, and "μ" and "ν"are dynamic and kinematic viscosity respectively. In the above equation $\frac{D}{Dt}$ *and* $\frac{d}{dt}$ is the material and time derivative respectively.

Interpretations of the terms used in the above equation are followings:

1. The first term represents the contribution of the pressure gradient of the flow on the force imposed by the flow on the particle, also known as pressure drag.

2. The second term is the added mass or virtual mass. This is an inertia imposed by the fluid as the accelerating particle has to move a volume of the surrounding body while it moves through the fluid.

3. The third term is the Stokes drag in the linear form. To achieve more accuracy we used in a nonlinear Stokes drag

$$-6\pi\mu a\left(V_i(t) - u_i[Y(t)],t\right)(1+\alpha)$$

Where, $\alpha = 0.15\,\mathrm{Re}_p^{0.687}$

$$\mathrm{Re}_p = 2a\,\mathrm{Re}|V - u|$$

Where “V” is the fluid velocity and “u” is the velocity of the particle.

3.4 Fluid Dynamics

A channel of size 4πh × 2h × 2πh is considered with dimensions streamwise “x”, wall normal direction “y”, and spanwise “z” direction respectively; with “h” being half channel height. Particles are injected in a turbulent flow with different initial velocities on a pseudo random pattern as the initial position. We solve the non-dimensional Navier-Stokes equations for incompressible viscous fluid.

In this thesis we have

$$\frac{\partial u}{\partial t} + (u \,.\, \nabla)u = -\nabla p + \frac{1}{\mathrm{Re}}\nabla^2 u \qquad \textbf{Equation 3-4}$$

$$\nabla .\, u = 0 \qquad \textbf{Equation 3-5}$$

The flow is defined by the non-dimensional parameter, Re. The flow is periodic in streamwise and spanwise directions and is driven by a time dependent pressure gradient. At the lower wall one applied the no slip boundary condition. The upper boundary of the domain can be treated as free surface with symmetry boundary condition for open channel and no slip boundary condition is used in case of poiseuille flow.

3.5 Governing equations for the swimmers

The flow is seeded with many particles, typically between 2×10^5 and 10^6. Swimmers are point particles which advected with the local flow velocity and the swimming speed u_s

$$\frac{dx_i}{dt} = u + u_s p \qquad \textbf{Equation 3-7}$$

In this expression, u is the local fluid velocity, $u_s = u_s(u, \nabla u)$ which may depend on local fluid velocity and shear and p is the local particle orientation. Note that one could modify the transport by including inertial effects, so that particles have a characteristic time scale to adjust to the local fluid velocity (this is zero for the expression above). This should not be the case for very small organisms.

To close the system one needs to define rules for u_s and an evolution equation for the orientation p. Assuming spheroid shape, the angular velocity of the organisms is defined by the inertia-free balance of gravitational and viscous torques. The deterministic part of the cells' rate of change of direction is given by

$$\dot{p} = \frac{1}{2B}\left[k - (k \cdot p)p\right] + \frac{1}{2}\omega \times p + \alpha_{\circ}(I - pp) \cdot E \cdot p \cdot \qquad \textbf{Equation 3-9}$$

The first term in the above equation describes the reorientation due to cells' being bottom heavy, k is unit vector in the vertical direction and B α $\mu/(\rho_p gh)$ is the gyrotactic reorientation parameter with h the distance between the centre of spheroid and its centre of mass. The second term represents reorientation due to viscous torque on the cell caused by vorticity "ω" and the third term is reorientation due to rate of strain of the linear shear flow, $\alpha_0 = (a^2 - b^2)/(a^2 + b^2)$ the eccentricity of the spheroids which is represented by l in the plots in chapter 5, and E symmetric part of the deformation tensor. Rotational diffusion is added as stochastic process of given mean and standard deviation.

We did the some cases with particles having zero velocity when injected in the fluid so the equation reduces to the following equation

$$\frac{dx_i}{dt} = u \qquad \textbf{Equation 3-10}$$

If the cells are symmetric not the bottom heavy, the gyrotactic reorientation parameter B will be equal to zero because "h" is equal to zero which is the distance between the centre of spheroid and its centre of mass. In this case the centre of spheroid and its centre of mass lie at

same the same point. For spherical cells a=b so α_0 will be equal to zero so that the rate of strain does not affect the orientation due to these the equation 3-9 reduces to

$$\dot{p} = \frac{1}{2}\omega \times p \qquad \textbf{Equation 3-11}$$

This shows that the reorientation due to viscous torque on the cell caused by vorticity "ω" But for the elongated shape having eccentricity equal to 1 and without gyrotaxis we have the following equation

$$\dot{p} = \frac{1}{2}\omega \times p + (I - pp) \cdot E \cdot p \cdot \qquad \textbf{Equation 3-12}$$

In this case, the first term represents reorientation due to viscous torque on the cell caused by vorticity "ω" and the second term is reorientation due to rate of strain of the linear shear flow.

Chapter 4

4.1 Numerical Simulation

We used a program called “SIMSON” for all simulations in our work. This solver is implemented in FORTRAN 77/90. An efficient spectral integration technique is used to solve the Navier Stokes equations for incompressible channel flows. We can run this program either as a solver for direct numerical simulations (DNS) in which all length and time scales are resolved or in large-eddy simulations (LES) mode where a number of different subgrid-scale models are available. The evaluation of multiple passive scalars can also be computed. The code can be run distributed or with shared memory parallelization through the Message Passing Interface (MPI) or OpenMP, respectively.

4.2 Fluid Phase

Equations for fluid are solved in spectral space, i.e. Fourier series for streamwise and spanwise directions and Chebyshev series for wall normal directions. Their results are transferred back to the physical space using backward Fourier and Chebyshev transformations. The streamwise and spanwise directions are spatically discretized using Fourier expansions, while Chebyshev polynomial on Gauss-Lobatto points is used for wall normal directions. For temporal integrations, two semi-implicit schemes are used. The third order Runge-Kutta (RK3) scheme is used for the integration of advection and forcing terms, while diffusive terms are integrated by an implicit second-order Crank-Nicolson scheme. The basic numerical method is similar to the Fourier-Chebyshev method used by Kim et al. (1987) classically used for canonical turbulent flows.

4.3 Particle Phase

Particle advection is also solved in SIMSON. Fluid velocity and its derivative must be known at the particle position for the calculation of the force at the particle. For that, the particle position is projected onto the horizontal planes, both above and beneath. On each horizontal plane four grid points surrounding the particle projections are found and fluid velocities are then interpolated from these grid points on to the particle projections using a second order

accurate linear interpolation. Then fluid velocities are interpolated onto the particle position using another linear interpolation, this time in wall normal direction.

For Particle integration we used the RK3 integration scheme, the same scheme that is used to integrate the fluid. For this particle equation of motion is solved at each of four RK sub steps and the interpolation of fluid velocities is taken at each sub step. Vorticity and velocity fields are used to get velocity gradients in Fourier space on each and every horizontal plane.

Chapter 5

5.1 Results and Discussions for Open Channel

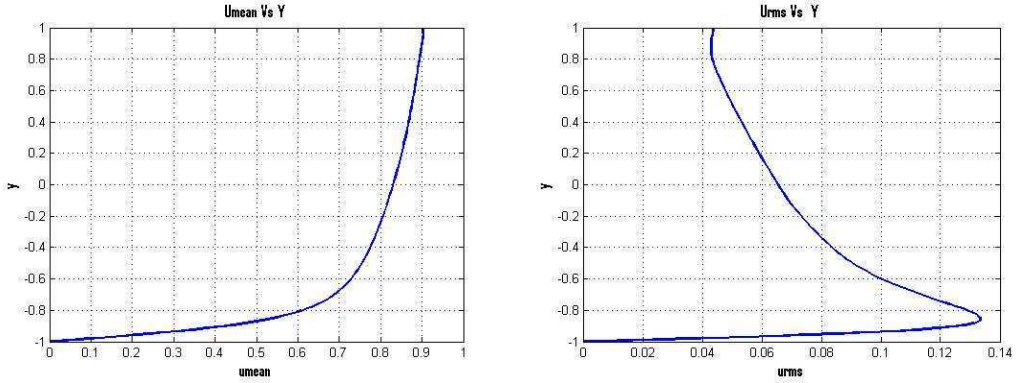

Figure 5-1: Statistics of turbulent flow. Left: mean streamwise velocity. Right: streamwise velocity fluctuations.

Here we report results for open channel flow with passive swimming particles. The flow is open channel, periodic in the streamwise and spanwise direction and delimited by a wall and a free surface in the vertical y direction. The friction Reynolds number is Re_τ = 74.246 and the domain size 4πh × 2h × 2πh. In figure 5-1 we report the mean velocity profile and the fluctuations of the streamwise velocity component u versus the wall-normal coordinate.

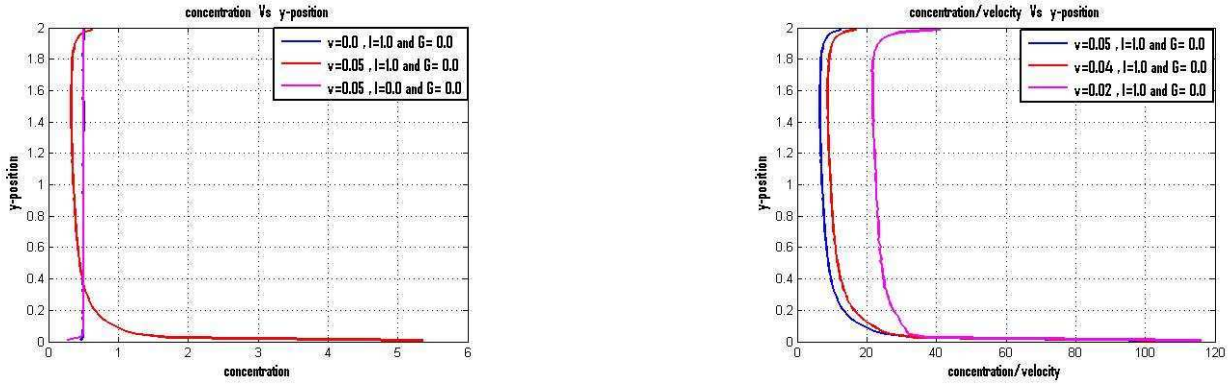

Figure 5-2: Concentration of swimmers across the channel. Left: Comparison between the three populations considered. Right: comparison for elongated swimmers of different swimming speed. The concentration is scaled by swimming speed to show linear scaling.

For the results presented here for the swimmers, random rotational diffusion is not considered. In figure 5-2 we show the wall-normal distribution of the normalized particle concentration. For the case of dead elongated particles (eccentricity 1) and for spherical particles swimming at u_s = 0.05 the concentration is uniform, as for passive tracers. Interestingly, elongated swimmers tend to accumulate at the lower wall. Simulations with lower values of the swimming speed show lower levels of accumulation. The concentration at the wall appears to be proportional to the swimming speed (see figure 5-2 right where the concentration is scaled by the swimming speed).

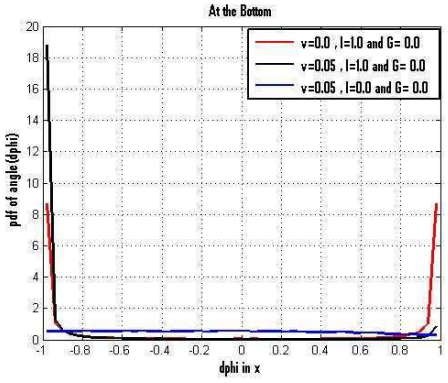

Figure 5-3: PDF of cosine between the swimmer orientation and the x-direction (streamwise direction).

The probability density function of the cosine of the angle between particle orientation and the streamwise direction is reported in figure 5-3 for particles located close to the wall. Dead elongated swimmers are aligned with the flow, equal probability for positive and negative orientation. Spherical swimmers show no preferential direction while elongated micro-organisms those are injected with initial velocity are swimming against the mean flow.

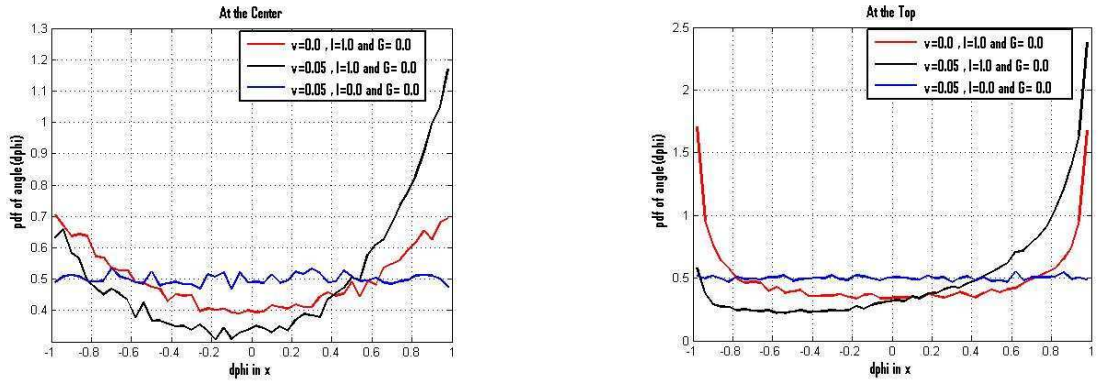

Figure 5-4 : PDF of cosine between the swimmer orientation and the x-direction (streamwise direction).

In figure 5-4 we showed the orientation for particles located at the centre of the channel and close to the free surface. A more uniform distribution is observed in this case: swimming prolate particles tend to align with the flow close to the free surface. The distribution of the orientation with respect to the spanwise and wall-normal directions does not show any peculiar behavior.

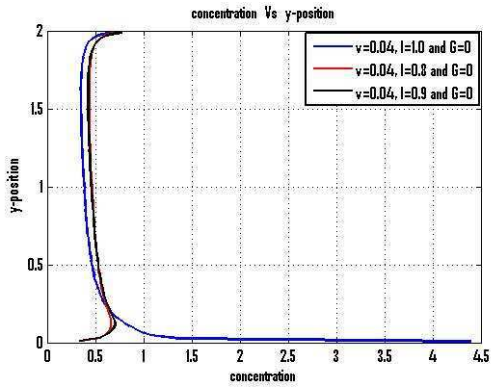

Figure 5-5: Concentration of swimmers across the channel. Comparison between the two populations.

In figure 5-5 we showed the wall-normal distribution of the normalized particle concentration. In this case all swimmers are injected with u_s = 0.04, elongated particles (eccentricity 1) tend to accumulate at the lower wall as shown earlier and the concentration of ellipsoid particles (eccentricity 0.8 and 0.9) seems uniform except at the wall due to large scale but if we look at the figure 5-8 this is not uniform at all.

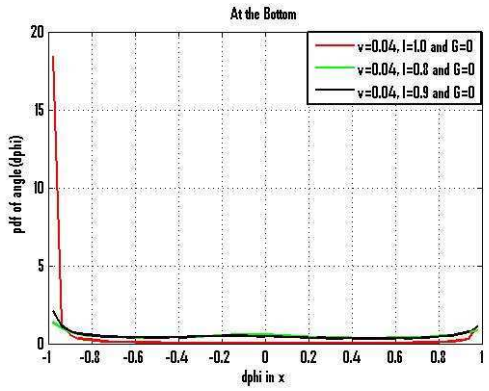

Figure 5-6 : PDF of cosine between the swimmer orientation and the x-direction (streamwise direction).

In figure 5-6, PDF of cosine between the swimmer orientation and the x-direction at the wall, ellipsoidal swimmers show no preferential direction while elongated swimmers are swimming against the mean flow.

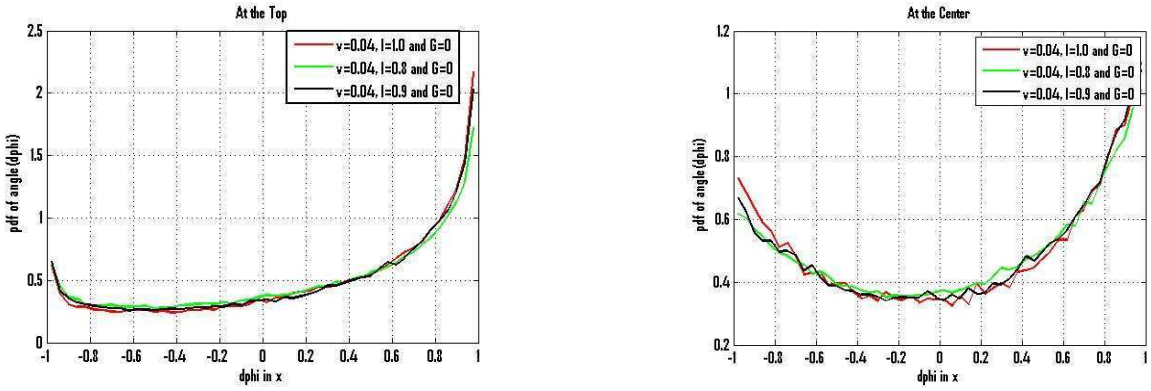

Figure 5-7 : PDF of cosine between the swimmer orientation and the x-direction (streamwise direction).

In figure 5-7, PDF of cosine between the swimmer orientation and the x-direction at the center and at the free surface. The ellipsoidal and the elongated swimmers show the same behavior. Swimmers of both shapes have more probability to move in the direction of mean flow at the top and at the center.

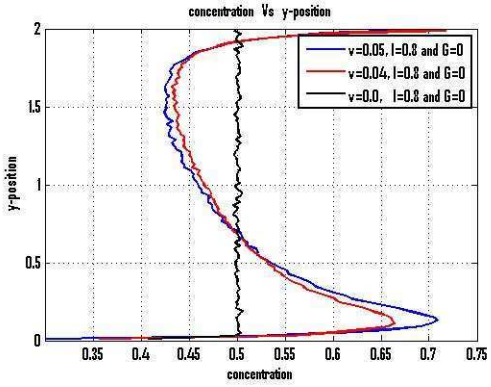

Figure 5-8: Concentration of swimmers across the channel.

In figure 5-8, the comparison of three different concentrations is presented when the ellipsoid particles with three different velocities are injected in the fluid. Particles those are injected with zero initial velocity have uniform concentration across the channel but the particles those are injected with some velocity are accumulated at the lower wall and upper surface.

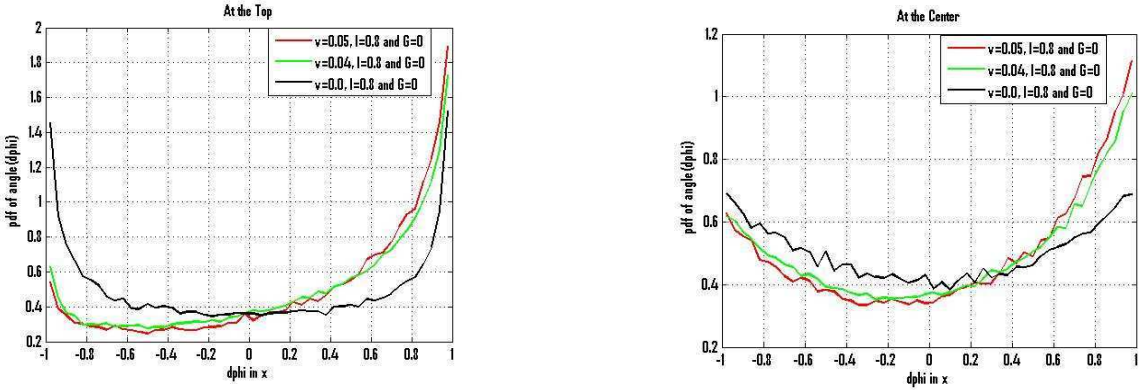

Figure 5-9 : PDF of cosine between the swimmer orientation and the x-direction (streamwise direction).

In figure 5-9, PDF of cosine between the swimmer orientation and the x-direction at the center and top, orientation of the swimmers at the top and bottom is same. Swimmers those are injected with zero velocity have equal probability for positive and negative orientation. Swimmers those are injected with some velocity have more probability to swim in direction with the mean flow.

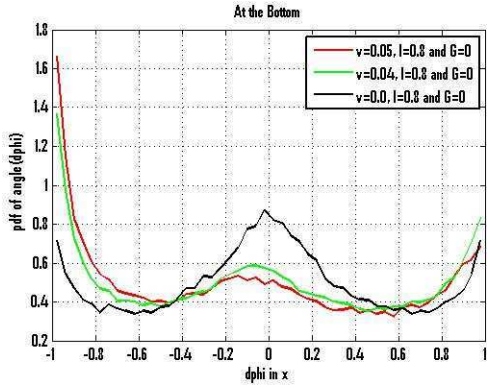

Figure 5-10: PDF of cosine between the swimmer orientation and the x-direction (streamwise direction).

In figure 5-10, PDF of cosine between the swimmer orientation and the x-direction at the wall, swimmers those are injected with zero velocity are normal to wall and to the mean flow velocity. They are symmetric with respect to the mean value. Swimmers those are injected with some velocity are mostly against the mean flow but have some probability of orientation normal to wall and to the mean flow.

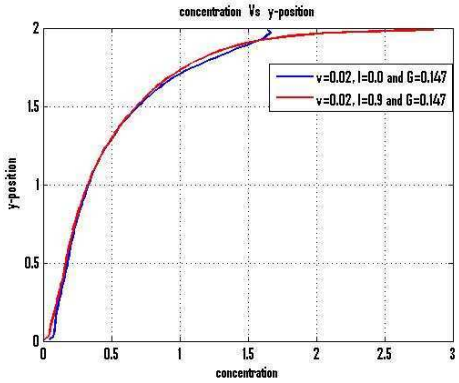

Figure 5-11: Concentration of swimmers across the channel.

In figure 5-11, the concentration comparison for spherical and ellipsoid gyrotactic swimmers is shown. Ellipsoid swimmers are accumulating at the surface more than the spherical swimmers. But for both cases swimmers are accumulating at the surface more than any other location.

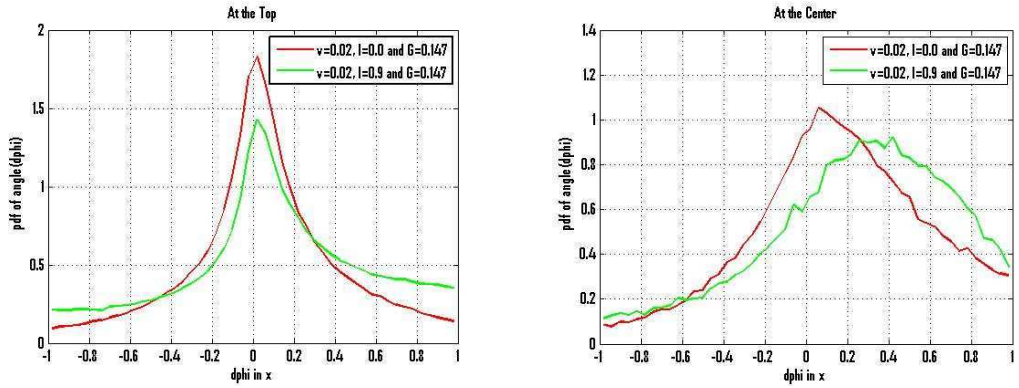

Figure 5-12 : PDF of cosine between the swimmer orientation and the x-direction (streamwise direction).

In figure 5-12, PDF of cosine between the swimmer orientation and the x-direction at the center and top, orientation of the swimmers at the top and bottom is almost same and most of the swimmers are normal to wall and to the mean flow velocity.

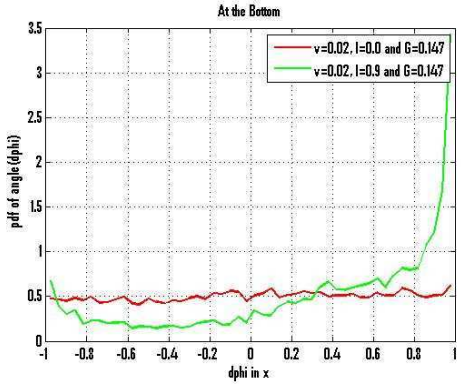

Figure 5-13 : PDF of cosine between the swimmer orientation and the x-direction (streamwise direction).

In figure 5-13, PDF of cosine between the swimmer orientation and the x-direction at the wall, gyrotactic spherical swimmers show no preferential direction while gyrotactic ellipsoid swimmers are moving with the mean flow.

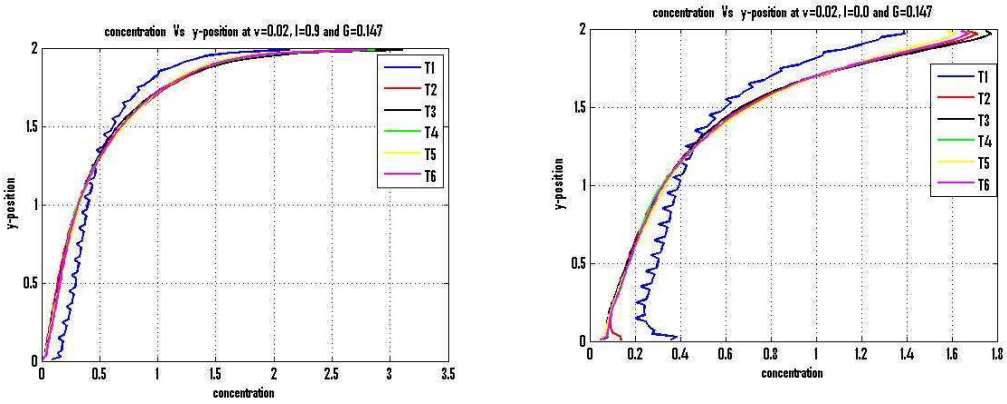

Figure 5-14: Concentration of gyrotactic swimmers across the channel.

In figure 5-14, the concentration of the gyrotactic swimmers is shown at different time steps. First they are not steady but after some time they became steady and accumulating at the upper surface.

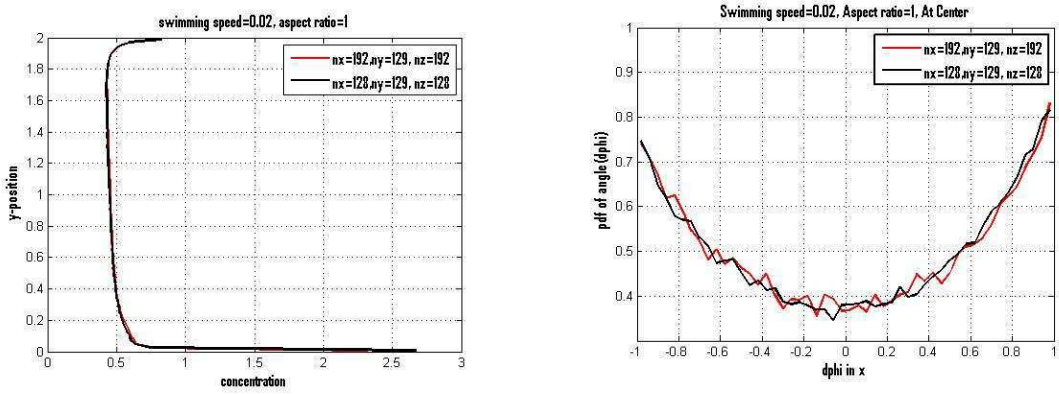

Figure 5-15: left-Concentration of swimmers across the channel. Right-Comparison for elongated particles at different resolution scale.

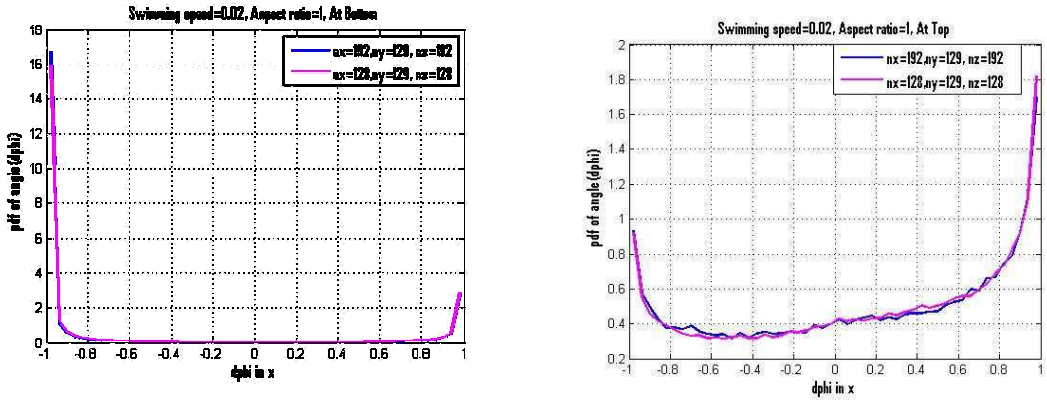

Figure 5-16 : PDF of cosine between the swimmer orientation and the x-direction (streamwise direction).

In the figures 5-15 and 5-16, we showed the dependence of concentration of the swimmers across the channel and pdf of cosines between their orientation and x-direction at two different resolutions $192 \times 129 \times 192$ and $128 \times 129 \times 128$ From the plots it is clear that there is no difference between the results at two resolutions. So all the results presented in future in the case of close channel are at $128 \times 129 \times 128$ this resolution to save the computation time.

5.2 Results and Discussions for Close Channel

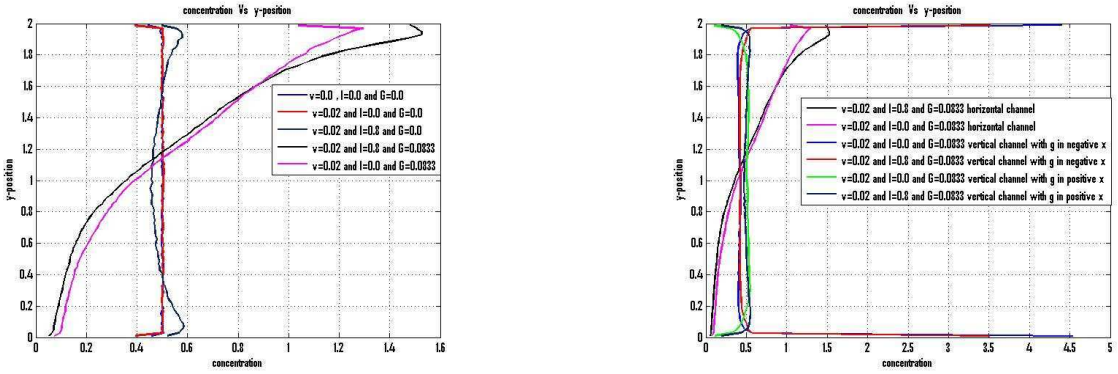

Figure 5-17: Concentration of gyrotactic swimmers in turbulent flow across the channel

In figure 5-17, left-we showed the concentration comparison of five different cases in the horizontal channel. Spherical swimmers without gyrotaxis are uniform across the channel while concentration of ellipsoid swimmers is non-uniform. Swimmers with gyrotaxis are tending to move up. Right-we showed the concentration comparison of gyrotactic swimmers in horizontal and vertical channel (with gravity in negative and positive x-direction). Swimmers in the vertical channel with gravity in negative x-direction are accumulating at the wall and away from the wall with gravity in positive x-direction while in horizontal they are tending to move up.

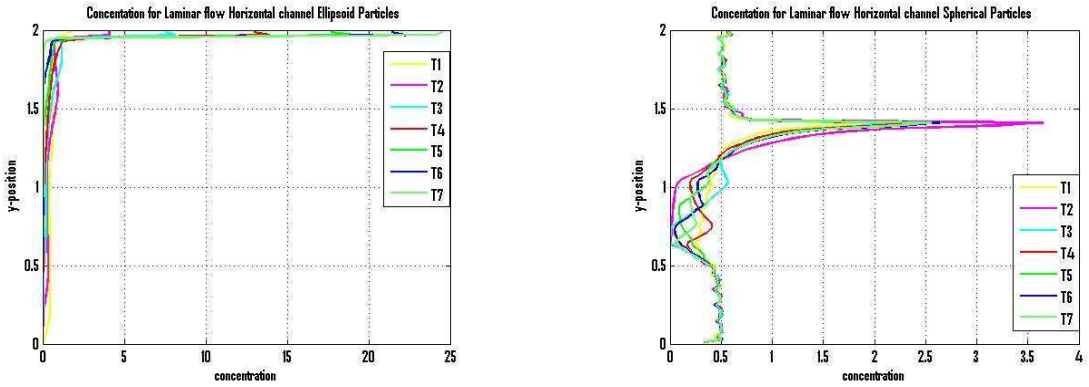

Figure 5-18: Concentration of gyrotactic swimmers in laminar flow across the channel

In figure 5-18, Left- the concentration of gyrotactic ellipsoid swimmers at different time steps is shown. In this case all the swimmers are accumulating at the upper wall. Right- the concentration of gyrotactic spherical swimmers is presented at different time step. In this case swimmers are accumulating at the distance of 0.6 from the upper wall.

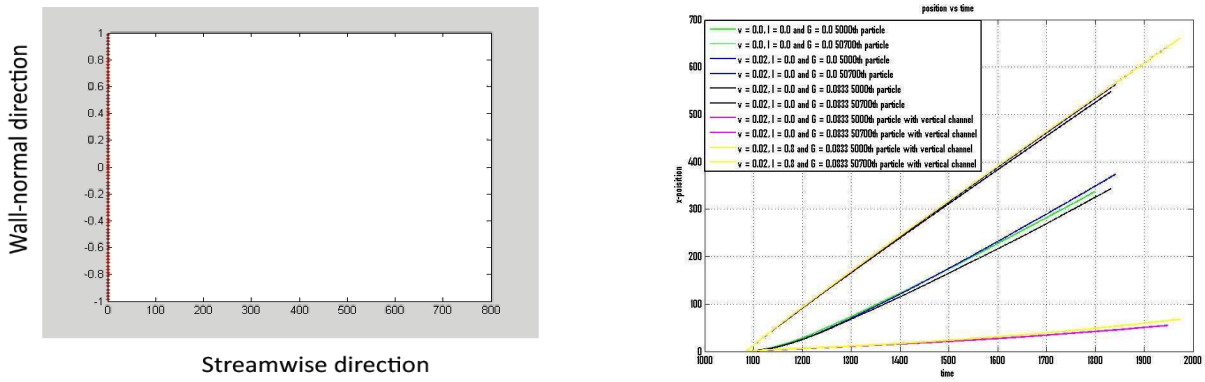

Figure 5-19: left-initial position of swimmers in the channel. Right- Computation of Dispersion Velocity

The figure 5-19, left shows that swimmers are localized in streamwise direction but the orientation of the swimmers is random. Figure at right is the position versus time plot for particle at 1% and 99% when ordered according to streamwise location (98% of swimmers within the delimited area). We computed the trailing and leading edge velocity of particle packet from linear interpolation after initial transient.

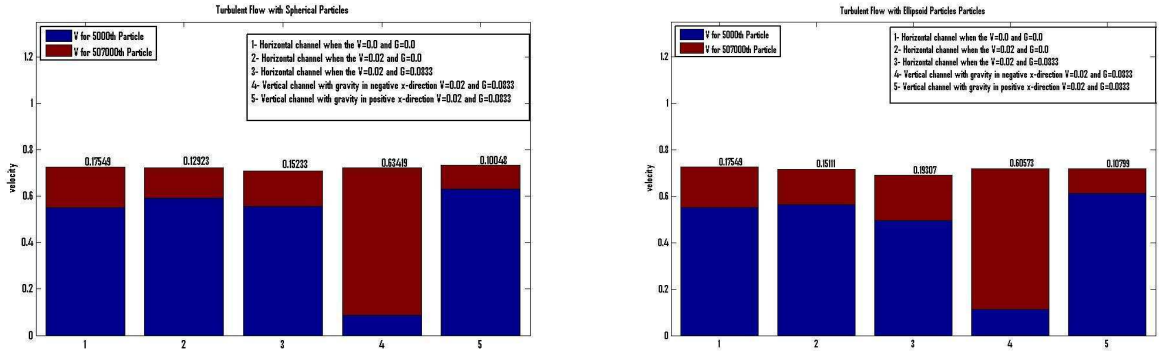

Figure 5-20: Computation of Dispersion Velocity in turbulent channel.

In figure 5-20, left plot is velocity dispersion for spherical swimmers in turbulent flow. For the case four when the channel is vertical and the gravity is in negative x-direction swimmers tend to migrate towards the wall and this yields the largest spreading. Right plot is the velocity dispersion for ellipsoid swimmers (eccentricity 0.8) the trend of these swimmers in same as the spherical swimmers with slightly larger dispersion. The values on the top of each bar are the difference between the interpolated velocity of the swimmers at the trailing and the leading edge.

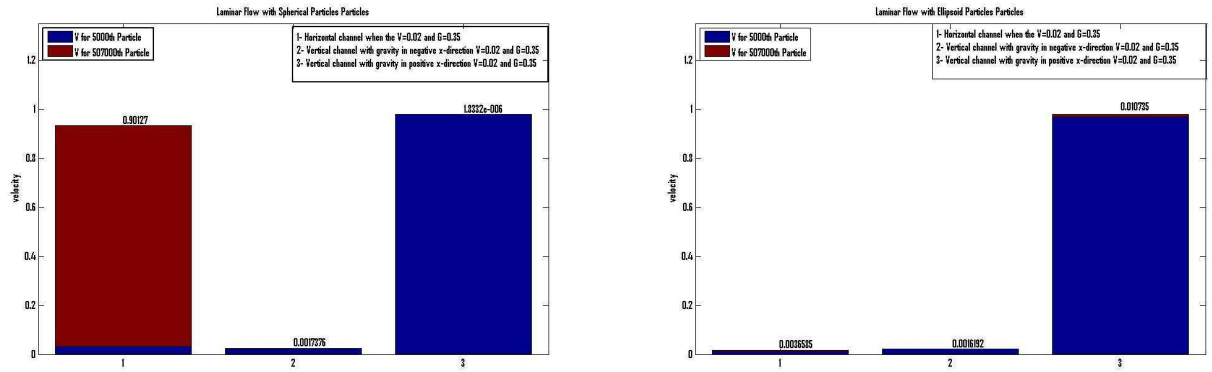

Figure 5-21: Computation of Dispersion Velocity in laminar channel

In figure 5-21, left-plot is velocity dispersion for spherical swimmers in laminar flow. Right-plot is the velocity dispersion for ellipsoid swimmers in laminar flow. In laminar case trend is not same for spherical and ellipsoid swimmers as we saw in turbulent case. We saw the maximum dispersion for vertical channel when the flow is against the gravity for both spherical and the ellipsoid swimmers. In these cases swimmers are accumulating at the both walls. While in the cases when the flow is in the direction of gravity swimmers are accumulating at the center of the channel. In horizontal channel spherical swimmers are moving with the flow but accumulating at the upper wall in case of ellipsoid swimmers.

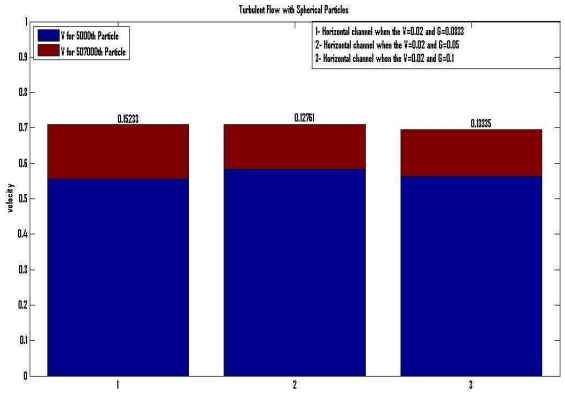

Figure 5-22: Computation of Dispersion Velocity in turbulent channel

In figure 5-22, we showed the dependence of dispersion velocity of spherical swimmers on gyrotactic parameter in turbulent flow when the channel is horizontal. Dispersion velocity increases with increase in gyrotactic value.

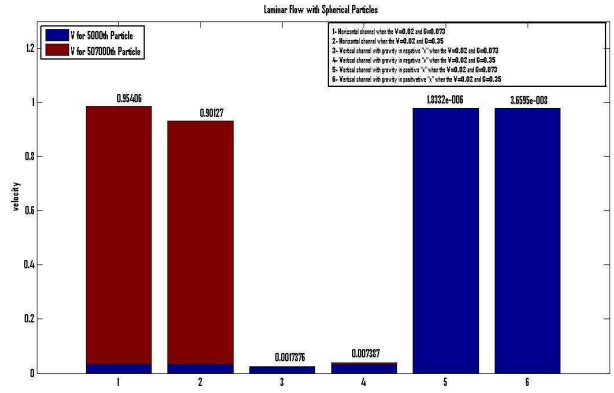

Figure 5-23: Computation of Dispersion Velocity in laminar channel

In figure 5-23, we showed the dependence of dispersion velocity of spherical swimmers on gyrotactic parameter in laminar flow. Trend for dispersion in all channels is same as observed previously in figure 5-21. In horizontal channel and the vertical channel with gravity in the positive x-direction with the increase in gyrotactic value the difference between the

interpolated velocities of the swimmers at the trailing and edge decreases but it increases in the case when the channel is vertical and the gravity is opposite to the direction of flow (negative x-direction).

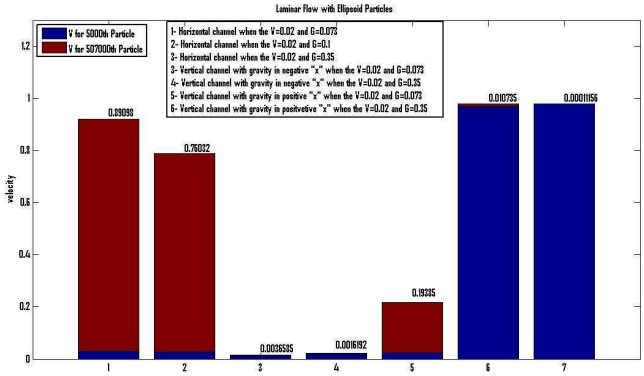

Figure 5-24: Computation of Dispersion Velocity in laminar channel

In figure 5-24, we showed the dependence of dispersion velocity of ellipsoid swimmers on gyrotactic parameter in laminar flow. Trend for dispersion in all channels is same as observed previously in figure 5-24. But there is big difference for the horizontal channel because all swimmers are accumulating at the wall as shown in figure 5-18(left). In horizontal channel and the vertical channel with gravity in the positive x-direction with the increase in gyrotactic value the difference between the interpolated velocities of the swimmers at the trailing and edge decreases but it increases in the case when the channel is vertical and the gravity is opposite to the direction of flow (negative x-direction).

Chapter 6

Conclusion

We used direct numerical simulations (DNS) for solution of microorganisms in channel flow. The swimmers are tracked in the flow by implementing a Lagrangian particle tracking (LPT) model for swimmers in the spectral simulation code called SIMSON. We have one way coupling so only the effect of flow on the microorganisms is considered but we neglected the response of swimmers on the flow. The results presented include the statistical analysis of swimmers concentration and their orientation in the open channel turbulent flow for Re_τ = 74.246. For close channel we reported the concentration and dispersion velocity of swimmers in turbulent flow at Re_τ = 180.

In the investigation of swimmers behavior in an open channel we found several interesting features. The concentration for spherical, dead ellipsoid and dead elongated microorganisms is almost uniform across the channel. Elongated swimmers are accumulating at the wall while the concentration of ellipsoid swimmers having some initial velocity is not uniform at all across the channel. Gyrotactic swimmers are accumulating at the upper surface which confirms the presence of gyrotaxis phenomena.

If we look at the orientation of the microorganisms at the wall, spherical swimmers showed no preferential direction while dead elongated swimmers have equal probability of positive and negative orientation. Dead ellipsoid swimmers are normal to wall and to the mean flow velocity. Elongated and ellipsoid swimmers those are injected with some initial velocity swim against the mean flow may be due to shear stress at the wall. Gyrotactic spherical swimmers have the same behavior observed for spherical swimmers without gyrotaxis but the gyrotactic ellipsoid swimmers are moving with the mean flow.

At the center and the free surface spherical swimmers showed no preferential direction same behavior observed at the wall but dead elongated and ellipsoid swimmers have equal probability of positive and negative orientation while elongated and ellipsoid swimmers with

and without gyrotaxis injected with some initial velocity have more probability to move in the direction of mean flow.

In close channel, for turbulent flow the concentration of spherical microorganisms without gyrotaxis is uniform across the horizontal channel, while the concentration of ellipsoid swimmers without gyrotaxis is not uniform across the horizontal channel. Microorganisms of both shape and gyrotaxis are tending to move and accumulating at the wall. Concentration of gyrotactic swimmers across the vertical channel when the gravity is in the direction of flow is almost uniform but the gyrotactic swimmers are accumulating at the wall when the gravity is on opposite direction of flow.

In laminar flow for horizontal channel at large gyrotactic value spherical swimmers are accumulating 0.6 units below from the upper wall while the ellipsoid swimmers are accumulating at the walls. For vertical channel when the gravity is in the same direction of flow the swimmers move towards the axis of the channel and accumulate there but when the gravity is in the opposite direction of flow microorganisms move towards the wall and accumulate there. These investigations are perfectly matched with the experimental results reported by John O. Kessler in 1986.

When we look at the velocity dispersion in different channel for turbulent flow, maximum velocity dispersion is observed for vertical channel when the gravity is in positive x-direction for spherical swimmers and slightly larger dispersion is observed for the ellipsoid swimmers as compared to spherical swimmers. We observed the same trend when the channel is vertical but the flow is laminar. In horizontal channel when the flow is turbulent dispersion velocity increases with increase in gyrotactic value.

Next step would be to study how cell patterns, e.g. accumulate at the wall and affect of turbulence

References:

1. The Orientation of Spheroidal Microorganisms Swimming in a Flow Field T. J. Pedley and J. O. Kessler Proc. R. Soc. Lond. B 1987 231, 47-70
2. Turbulent Flows by Stephen B. Pope
3. Microorganisms by Sundara Rajan S.
4. A First Course in Turbulence by H. Tennekes and J.L. Lumley
5. http://science.yourdictionary.com/organism
6. *http://en.wikipedia.org/wiki/Rheotaxis*
7. Mathew M. Hopkinsi And LiSA J. Fauci J., A Computational Model Of The Collective Fluid Dynamics Of Motile Microorganisms, Fluid Mech. (2002), vol. 455, pp. 149–174. 2002 Cambridge University Press.
8. S. Ghorai and N. A. Hill, Periodic Arrays Of Gyrotactic Plumes In Bioconvection, Department of Applied Mathematics, University of Leeds, Leeds LS2 9JT, United Kingdom (Received 7 December 1998; accepted 23 September 1999)
9. S. Ghorai and N. A. Hill, Gyrotactic Bioconvection In Three Dimensions, (Received 6 September 2006; accepted 23 March 2007; published online 17 May 2007)
10. Martin A. Bees And Ottavio A. Croze, Dispersion Of Biased Swimming Micro-organisms In A Fluid Flowing Through A Tube, doi: 10.1098/rspa.2009.0606
11. O A Croze, E E Ashraf and M A Bees, Sheared Bioconvection In A Horizontal Tube, doi:10.1088/1478-3975/7/4/046001
12. T. J. Pedley And J. O. Kessler, Hydrodynamic Phenomena In Suspension Of Swimming Microorganisms, Annual Review of Fluid Mechanics, Vol. 24: 313 -358 (Volume publication date January 1992).
13. S. Elghobashi, “On Predicting Particle-laden Turbulent Flows”, Applied Scientific Research, 52, 309-329 (1994)

14. M.R. Maxey and J.Riley, Equation Of Motion For A Small Rigid Sphere In A Nonuniform flow, Phys. Fluids 26, 883 (1983).
15. Alireza Farahanikia, Forces on Lagrangian Particles in Turbulent Wall-Bounded Flow, Master Thesis At KTH, 2010.